

# Electrochemical Immunosensor for Detection of Prostate Specific Antigen Based on CNSs/Thi@AuNPs Nanocomposites as Sensing Platform

Lihua Li<sup>1,#</sup>, Shengpeng Zhang<sup>1,#</sup>, Lizhen Yu<sup>1</sup>, Wenzhi Zhang<sup>1</sup>, Yan Wei<sup>1,2</sup>, Dexiang Feng<sup>1,2,\*</sup>

<sup>1</sup> Department of Pharmacy, Wannan Medical College, Wuhu, 241002, China

<sup>2</sup> Institute of Synthesis and Application of Medical Materials, Department of Chemistry, Wannan Medical College, Wuhu, 241002, China

\*E-mail: [fengdxiang@163.com](mailto:fengdxiang@163.com)

#These authors contributed equally to this work

Received: 6 January 2022 / Accepted: 4 June 2022 / Published: 4 July 2022

A sensitive immunosensor for quantifying prostate specific antigen (PSA) had been described. In the design, gold nanoparticles decorated thionine-functionalized carbon nanospheres (CNSs/Thi@AuNPs) for immobilization of primary antibody (Ab<sub>1</sub>) as an electrochemical sensing platform. Silicon dioxide nanospheres (SiO<sub>2</sub> NSs), with large surface area and good biocompatible, were loaded with horseradish peroxidase (HRP) and horseradish peroxidase labeled secondary antibodies (HRP-Ab<sub>2</sub>). In the presence of PSA, a sandwich type immunocomplex from Ab<sub>1</sub>-Ag-Ab<sub>2</sub> had been formed. Differential pulse voltammetry (DPV) was employed to obtain the response signal of immunosensor. Under the suitable experimental conditions, the changes of current intensity were linear with the logarithm of PSA concentration from 0.1 pg·mL<sup>-1</sup> to 100 ng·mL<sup>-1</sup>, and the detection limit was 0.025 pg·mL<sup>-1</sup> (S/N=3). Moreover, the immunosensor possessed satisfactory specificity, repeatability and stability, suggesting that it had potential application value in the detection of tumor markers.

**Keywords:** Electrochemical immunosensor; Prostate specific antigen; Horseradish peroxidase; Silicon dioxide nanospheres; CNSs/Thi@AuNPs nanocomposites

## 1. INTRODUCTION

Prostate cancer (PCa) represents one of the most common forms of cancer affecting men worldwide and is particularly prevalent among men of age 50 and older [1,2]. Primary PCa has no obvious clinical manifestation. This makes early diagnosis important for successful cancer treatment [3]. Prostate specific antigen (PSA), a glycoprotein almost entirely secreted by the prostate gland, is recognized as an important tumor marker for the diagnosis, monitoring, and risk prediction of PCa [4-6]. In general, the serum level of PSA in normal men is less than 4 ng·mL<sup>-1</sup>, if it exceeds 10 ng·mL<sup>-1</sup>, the patient is likely to develop prostate cancer [7-9]. Therefore, the development of a simple and effective

PSA test for detecting early asymptomatic PCa will be crucial to increase the chances of cure and reduce its mortality.

Conventionally, the PSA detection is based on immunoassay methods such as enzyme-linked immunosorbent assays (ELISA), radioimmunoassay, chemiluminescence, fluorescence and electrochemical immunoassay [10-13]. Among them, electrochemical immunoassay has attracted much attention due to its rapid, high sensitivity, and specificity, which provides a possibility for rapid and accurate screening and diagnosis of PCa in early stage.

However, the growing need for early and ultrasensitive surveillance of disease-related biomarkers is driving the development of biomarker sensitive assays through signal amplification. Fortunately, recent achievements in nanomaterials and nanotechnology have provided new avenues to develop novel signal amplification strategies for ultrasensitive immunoassay [14-16]. Because of their small size, large specific surface area and good stability at high temperatures, nanoparticles have been widely used for signal amplification including colloidal gold nanoparticles (AuNPs), magnetic nanoparticles (MNPs), carbon nanospheres (CNSs), quantum dots (QDs), silicon dioxide nanospheres (SiO<sub>2</sub> NSs) [17-21]. More importantly, the surfaces of these nanoparticles can be modified with oligonucleotides, enzymes, or antibodies to generate biological conjugates that serve as analysis cores and enhance signal generation by producing a synergistic effect to achieve higher sensitivity and lower detection limits [22,23].

Compared with a variety of nanoparticles, CNSs, AuNPs, SiO<sub>2</sub> NSs and their nanocomposites serve as signal amplification systems have many advantages: (i) they are nontoxic and highly biocompatible with biological systems; (ii) easy to be prepared and their surface can be functionally treated as needed [24-26].

In the present study, a sensitive electrochemical immunosensor was designed for PSA detection. Thionine (Thi), AuNPs and primary antibody (Ab<sub>1</sub>) were assembled on CNSs respectively to form CNSs/Thi@AuNPs nanocomposites, which not only served as sensing platforms, but also owned large surface area and good biocompatibility, and could load more signal molecules and antibodies to enhance response signal. SiO<sub>2</sub> NSs was used as a carrier for the immobilization of HRP and HRP labeled secondary antibody (HRP-Ab<sub>2</sub>). Sandwich-type immunocomplexes were formed when antibodies and antigens performed specific recognition responses. Meanwhile, in the medium containing H<sub>2</sub>O<sub>2</sub>, the prepared HRP-Ab<sub>2</sub>-SiO<sub>2</sub> NSs bioconjugate acted as a catalytic system with the help of thionine, further amplifying the reaction signal [27]. The experimental results showed the designed immunosensor had a wide linear range and high sensitivity. In addition, the detection results of serum samples by the developed method agreed well with ELISA values.

## 2. EXPERIMENTAL

### 2.1. Materials and Apparatus

Horseradish peroxidase (HRP), HRP-labeled monoclonal anti-PSA antibody (HRP-Ab<sub>2</sub>), PSA ELISA kit were purchased from Biocell Co., Ltd. carboxylated-carbon nanospheres (COOH-CNSs) were purchased from Xfnano Co., Ltd. 3-Aminopropyltriethoxysilane (APTES), Tetraethoxysilane

(TEOS), Thionine(Thi), Bovine serum albumin (BSA) were purchased from Aladdin Chemistry Co., Ltd. Other reagents were analytical grade, purchased from Sinopharm Chemical Reagent Co., Ltd. Twice-quartz-distilled water was used in all tests.

The morphology and the size of nanomaterials were measured on a scanning electron microscope (SEM, Hitachi, Japan). FTIR spectra of SiO<sub>2</sub> NSs and functionalization were obtained on an IR-21 spectrometer (Shimadzu, Japan). UV-vis absorption spectra were obtained on a U-5100 UV-vis-NIR spectrometer (Hitachi, Japan). Electrochemical measurements were carried out on CHI650C three-electrode electrochemical working system (Shanghai CH Instruments Co., China).

## 2.2. Preparation and functionalization of SiO<sub>2</sub> NSs

The preparation and surface functionalization of SiO<sub>2</sub> NSs were carried out according to reference [28,29]. 2.7 mL ammonium hydroxide and 5.0 mL deionized water were mixed with 90 mL ethanol, then 2.3 mL of TEOS was added into the mixture and stirred vigorously for 24 h. The white suspension was centrifuged, washed with ethanol for three times and dried to obtain monodisperse silica nanoparticles. 20 mg of SiO<sub>2</sub> NSs was then dispersed in 50 mL ethanol and treated with 0.4 mL APTS. After being stirred for 6 h, the suspension was washed three times and the amino-functionalized SiO<sub>2</sub> NSs (NH<sub>2</sub>-SiO<sub>2</sub> NSs) were obtained. Next, NH<sub>2</sub>-SiO<sub>2</sub> NSs (20 mg) were suspended in 20 mL of N, N-Dimethylformamide (DMF) containing 0.1 mol·L<sup>-1</sup> glutaric anhydride by ultrasonic stirring for 10 min and reacted 24 h under magnetic stirring. The centrifuged precipitates were washed alternately with DMF and water three times to obtain carboxyl-functionalized SiO<sub>2</sub> NSs (COOH-SiO<sub>2</sub> NSs).

## 2.3. Preparation of HRP-Ab<sub>2</sub>-SiO<sub>2</sub> NSs bioconjugate

20 mg of COOH-SiO<sub>2</sub> NSs were ultrasonically dispersed in PBS solution (2 mL, pH 7.4) and activated with 2.6 mg EDC and 2.6 mg NHS for 30 min. Then, HRP (0.3 mL, 0.5 mg · mL<sup>-1</sup>) and HRP-Ab<sub>2</sub> (0.1 mL, 1.0 mg · mL<sup>-1</sup>) were added to the dispersion and stirred overnight at room temperature. The excessive enzymes and secondary antibodies were removed by centrifugation. The sediment was washed with PBS and re-dispersed in 2.0 mL PBS containing 1% BSA, which was stored in a refrigerator at 4°C for later use.

## 2.4. Preparation of CNSs/Thi@AuNPs

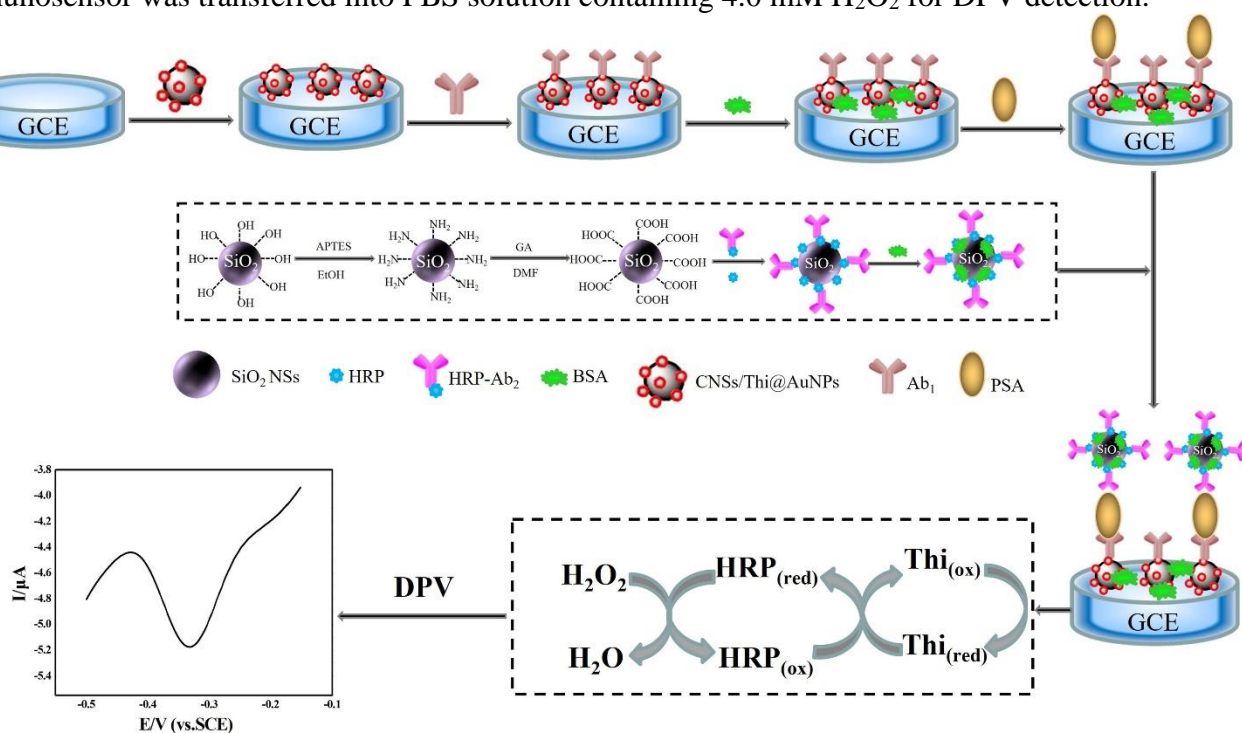
The preparation of CNSs/Thi@AuNPs nanocomposites referred to the method we introduced before [30]. Briefly, 1.0 mg carboxylated-CNSs were ultrasonically dispersed in 2 mL of distilled water and activated for 30 min by adding EDC and NHS to the suspension. Next, 2.0 mL Thi (1.0 mM) was added to the mixture and stirred for 12 h. After centrifugation, the precipitate was washed three times, and slowly dropped into AuNPs solution (10.0 mL) with mild agitation for another 12 h. Finally, the mixture was centrifuged, washed and dispersed in PBS (2.0 mL, pH 7.0).

### 2.5. Fabricating immunosensor

The glassy carbon electrode (GCE) was repeatedly polished with 0.05 $\mu\text{m}$  aluminum powder, ultrasonically cleaned with water and ethanol, and then blow-dried with nitrogen. 10  $\mu\text{L}$  CNSs/Thi@AuNPs nanocomposites were dribbled onto the surface of GCE and dried naturally at room temperature. The decorated electrode was immersed in PSA primary antibodies ( $\text{Ab}_1$ , 200  $\mu\text{g} \cdot \text{mL}^{-1}$ ) and incubated at 37  $^\circ\text{C}$  for 12 h. Finally, the electrode was blocked with 1 % BSA at 37 $^\circ\text{C}$  for 45 min.

### 2.6. Detection of PSA

PSA testing protocol was shown in scheme 1. Firstly, the prepared immunosensor was incubated with PSA solution of different concentration for 50 min. After washing with PBS, the immunosensor was placed into HRP- $\text{Ab}_2$ - $\text{SiO}_2$  NSs bioconjugate for further incubation for 50 min. Then the immunosensor was transferred into PBS solution containing 4.0 mM  $\text{H}_2\text{O}_2$  for DPV detection.



**Scheme 1.** The construction process of immunosensor for electrochemical detection of PSA.

## 3. RESULTS AND DISCUSSION

### 3.1. Characterizations of $\text{SiO}_2$ NSs and HRP- $\text{Ab}_2$ - $\text{SiO}_2$ NSs bioconjugate

The shape of  $\text{SiO}_2$  NSs and its functionalization were investigated by SEM and FTIR. Figure. 1A showed SEM image of the  $\text{SiO}_2$  NSs. It could be observed that the  $\text{SiO}_2$  NSs had uniform spherical shape with an average size of  $\sim 300$  nm in diameter. Surface modification of  $\text{SiO}_2$  NSs was often used in immunoassay. In this work, surface functionalization of  $\text{SiO}_2$  NSs was carried out in two steps. Firstly, the amine groups were introduced on the surface of  $\text{SiO}_2$  NSs through silanization reaction by APTES,

and then the carboxyl groups were obtained by the extension reaction of amine groups and glutaric anhydride with a ring-opening linker [31]. FTIR spectra (Seen in Figure. 1B) confirmed the existence of amino and carboxyl groups on the surface of SiO<sub>2</sub> NSs after functionalization.

UV-vis spectrophotometry was employed to characterize the HRP-Ab<sub>2</sub>-SiO<sub>2</sub> NSs bioconjugate. From Figure. 1C, it could be observed that the bioconjugate appeared two new obvious absorptive peaks at 280 nm and 402 nm, which came from Ab<sub>2</sub> and HRP, indicating that HRP-Ab<sub>2</sub> and HRP were successfully bonded to SiO<sub>2</sub> NSs via the EDC/NHS method.

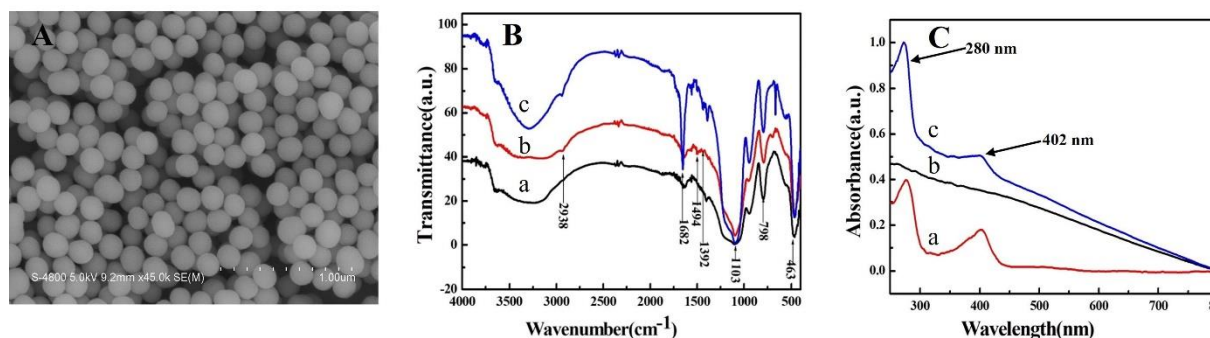


**Figure 1.** (A) SEM image of SiO<sub>2</sub> NSs. (B) FTIR spectra of (a) SiO<sub>2</sub> NSs, (b) NH<sub>2</sub>-SiO<sub>2</sub> NSs, (c) COOH-SiO<sub>2</sub> NSs. (C) UV-vis absorption of (a) HRP-Ab<sub>2</sub>, (b) SiO<sub>2</sub> NSs, (c) HRP-Ab<sub>2</sub>-SiO<sub>2</sub> NSs.

### 3.2. Characterizations of CNSs and CNSs/Thi@AuNPs

The surface morphology of CNSs and CNSs/Thi@AuNPs was characterized by SEM. As can be seen from Figure. 2A that CNSs was spherical with a diameter of 300-400 nm. When Thi and AuNPs were decorated on CNSs, a large number of “bright spots” could be seen on the surface of CNSs, meanwhile, EDX analysis confirmed the presence of Au element (seen Figure. 2B and 2C). Here, CNSs/Thi@AuNPs nanocomposites not only provided electrochemical signal as electron transport medium, but also improved the electrical conductivity of the electrode. Importantly, the incorporation of significant biocompatibility and high conductivity of AuNPs could further enhance the electrochemical signal and capture more primary antibodies.

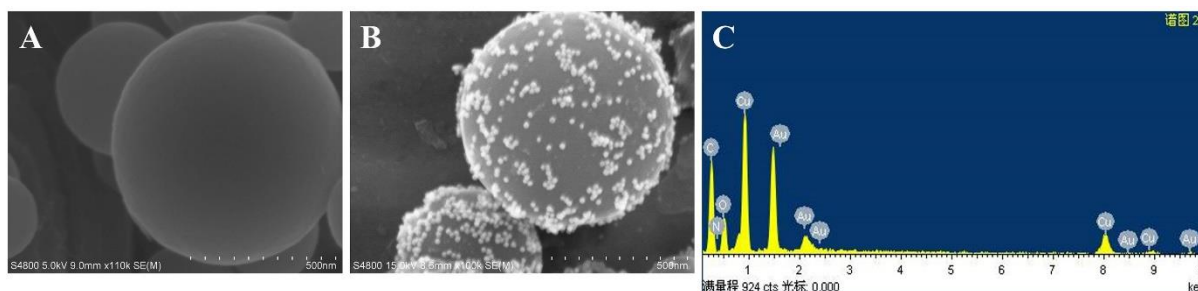


**Figure 2.** (A) SEM image of CNSs. (B) SEM image of CNSs/Thi@AuNPs. (C) EDX analysis of CNSs/Thi@AuNPs.

### 3.3. EIS and CV investigations of the immunosensor

The assembly process of immunosensor was studied by electrochemical impedance spectroscopy (EIS) and cyclic voltammetry (CV). EIS consists of a linear section representing the diffusion limiting process and a semicircular section reflecting the size of the electron transfer resistance ( $R_{et}$ ) [32]. After the bare GCE was modified by CNSs/Thi@AuNPs with excellent conductivity, the electron transfer was strengthened, and the  $R_{et}$  value decreased significantly (Figure. 3A, curve b). However, after coating Ab<sub>1</sub>, BSA and antigens on the electrode, the resistance increased successively (curve c, d and e), indicating that the presence of these bioactive substances impeded the electron transfer between the electrode and the alkaline solution. In addition, the test results of CV technique were consistent with those of EIS (showed in Figure. 3B).

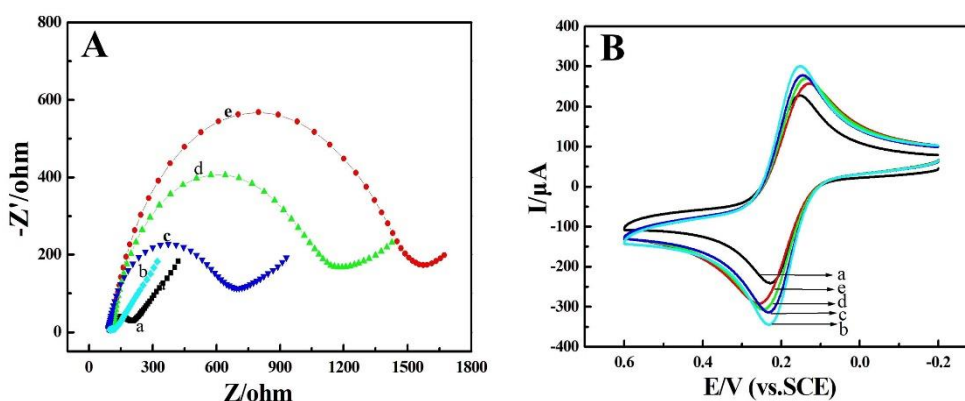


**Figure 3.** (A) EIS of (a) bare GCE, (b) CNSs/Thi@AuNPs/GCE, (c) Ab<sub>1</sub>/CNSs/Thi@AuNPs/GCE, (d) BSA/Ab<sub>1</sub>/CNSs/Thi@AuNPs/GCE, (e) antigens/BSA/Ab<sub>1</sub>/CNSs/Thi@AuNPs/GCE in 5 mM  $[\text{Fe}(\text{CN})_6]^{3-/4-}$  and 0.1 M KCl solution. (B) CV responses of the different modified electrodes in 1mM  $[\text{Fe}(\text{CN})_6]^{3-/4-}$  and 0.1 M KCl solution.

### 3.4. Optimization of experimental conditions

In order to obtain good performance of immunoassay, some experiment conditions were optimized. Because of the activity of HRP and the stability of antibody were related to the pH of solution, we researched the impact of pH on the response signal of the immunoassay. The result of Figure. 4A showed that with the increase of pH from 4.5 to 8.0, the peak current first increased and then decreased, reaching its maximum value at pH 6.5. Therefore, we selected the solution of pH 6.5 for the immunoassay.

The effect of the incubation time of secondary antibody and antigen on signal intensity was also investigated. As shown in Figure. 4B, in the range of 20-100 min, the peak current displayed its maximum when the time reached 50 min. Therefore, the electrochemical measurements were performed at incubation time of 50 min.

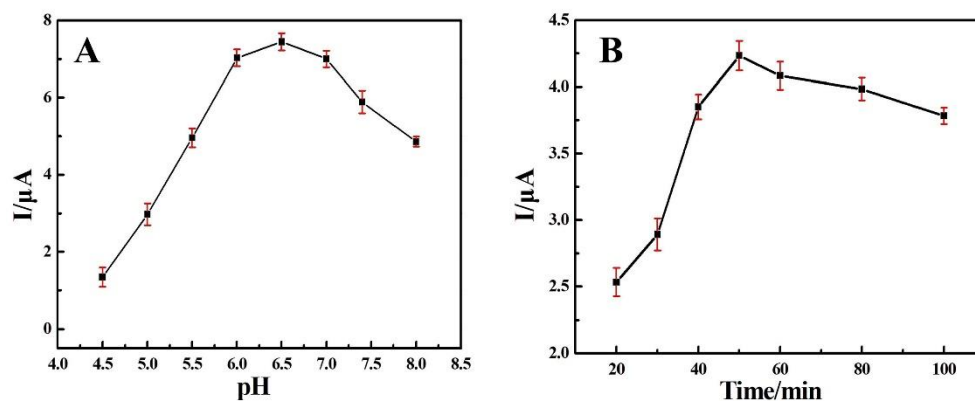


**Figure 4.** The influences of (A) pH, (B) incubation time on the current intensity of immunosensor.

### 3.5. Analytical performance

The quantitative range of the immunosensor was assessed under the optimum conditions. As can be seen from Figure. 5, with the increase of PSA concentration, the peak current of DPV enhanced gradually and a good calibration curve was obtained in the range of  $0.1 \text{ pg}\cdot\text{mL}^{-1}$  to  $100 \text{ ng}\cdot\text{mL}^{-1}$ .  $y(\mu\text{A}) = 5.1058 + 0.1198x(\text{ng}\cdot\text{mL}^{-1})$  was a linear regression equation, and its linear regression coefficient was 0.9951. The detection limit was estimated to be  $0.025 \text{ pg}\cdot\text{mL}^{-1}$  ( $S/N=3$ ). Compared with other PSA electrochemical immunosensors, our developed immunosensor showed higher sensitivity and satisfactory detection range (seen in Table. 1)[8,33-38], which may be attributed to the following aspects: First, AuNPs interspersed on the surface of CNSs not only improved the conductivity and electron transport capacity, but also increased the specific surface area, which can bind more primary antibodies [27]. Second, the modified  $\text{SiO}_2$  NSs had stable performance, good biocompatibility and large surface area, can load more HRP and secondary antibodies, enhanced the catalytic ability of signal molecule reaction, and enhanced the binding ability between antibodies and antigens.

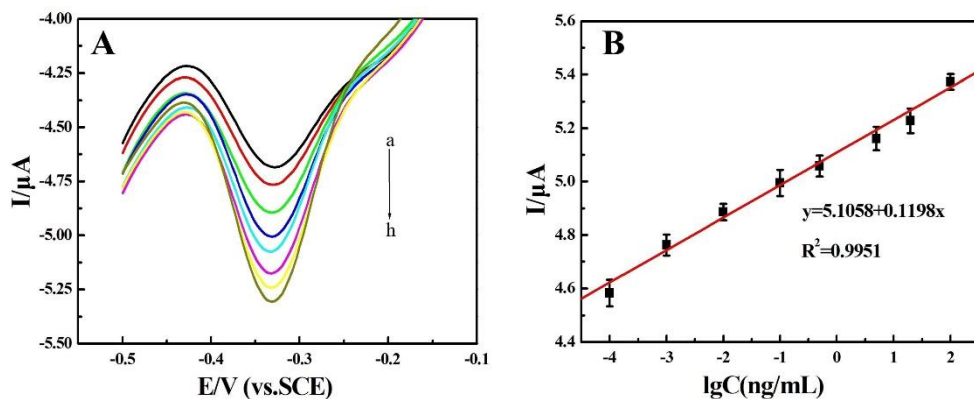


**Figure 5.** (A) DPV signals of the immunosensor with target PSA concentration of 0.0001, 0.001, 0.01, 0.1, 0.5, 5, 20, 100  $\text{ng}\cdot\text{mL}^{-1}$  (a~h) in PBS (pH 6.5). (B) The calibration curve of peak current vs. logarithm of PSA concentration.

### 3.6. Specificity, reproducibility and stability

In order to assess the specificity of the sensor, several possible interfering substances such as AFP, CEA, ascorbic acid (AA) and BSA were selected for detection [39]. The results (seen in Figure.6) showed that compared with the target analyte, the addition of the above substances had no significant effect on DPV signals, indicating that the sensor exhibited excellent selectivity.

Furthermore, PSA were measured with five parallel electrodes to investigate the repeatability of the sensor under the same conditions. The results showed a relative standard deviation (RSD) of 3.6 %. The immunosensor was stored in a refrigerator at 4°C for 3 weeks to dynamically investigate its stability. After one, two and three weeks, the DPV response signals of the immunosensor still maintained 96.5%, 94.2% and 91.6% of the initial levels.

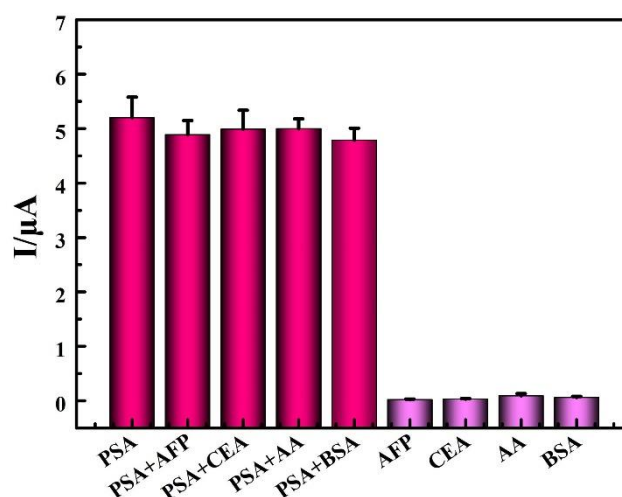


**Figure 6.** Specificity of the immunosensor.  $C_{PSA} = 20 \text{ ng} \cdot \text{mL}^{-1}$ ;  $C_{\text{interferents}} = 100 \text{ ng} \cdot \text{mL}^{-1}$ .

### 3.7. Samples analysis

To explore the feasibility of practical application of this method, eight human serum samples from Yiji Shan Hospital (Wuhu, China) were detected by the proposed and ELISA methods. The results were compared with the reference values obtained from the ELISA method (seen in Table. 2). The relative deviations were within -3.65% to 4.94 %, implying that the results obtained by the proposed method were basically consistent with those obtained by the ELISA.

**Table 1.** Comparison of analytical performance of various immunosensors for PSA

Electrode	Linear range ( $\text{ng} \cdot \text{mL}^{-1}$ )	Detection limit ( $\text{pg} \cdot \text{mL}^{-1}$ )	Refs
APBA/6-PICA/GCE	0.5-100	110	[8]
Au@Pt AuNCs/GCE	0.1-50	78	[33]
Br-Py/AuNP-Hep-Nafion/GCE	0.1-50	80	[34]

AgEPG/GCE	1-35	440	[35]
AuNPs/CHI/SPE	1-18	1	[36]
AuNPs@MWCNTs-GODs/GCE	1-10	0.48	[37]
AuNSs/FTO	0.05-30	5.7	[38]
CNSs/Thi@AuNPs/GCE	0.0001-100	0.025	This work

APBA, aminophenylboronic; 6-PICA, poly-indole-6-carboxylic acid; GCE, glassy carbon electrode; Au@Pt AuNC, gold/palladium bimetallic core-shell@gold nanocrystals; Br-Py, pyridinium bromide; AuNP, gold nanoparticle; Hep, heparin; AgEPG, silver nanoparticle-embedded porous graphene; CHI, chitosan; SPE, screen printed electrode; MWCNTs, multiwall carbon nanotubes; GODs, graphene quantum dots; AuNSs, gold nanostructures; FTO, fluorine-doped tin oxide.

**Table 2.** Comparison results of serum samples using the proposed and ELISA methods

Serum sample	Proposed method <sup>a</sup> (ng·mL <sup>-1</sup> )	ELISA <sup>a</sup> (ng·mL <sup>-1</sup> )	Relative deviation (%)
1	1.326±0.008	1.266±0.012	4.74
2	0.615±0.014	0.598±0.018	2.84
3	5.108±0.022	5.231±0.027	-2.35
4	2.486±0.009	2.369±0.012	4.94
5	1.925±0.015	2.002±0.011	-3.65
6	11.128±0.106	10.613±0.188	4.85
7	24.362±0.491	23.585±0.615	3.29
8	38.118±0.616	39.439±0.802	-3.35

<sup>a</sup> Mean value±SD of five measurements serum sample.

#### 4. CONCLUSIONS

In conclusion, an electrochemical immunosensor for quantitative detection of PSA had been developed. CNSs/Thi@AuNPs nanocomposites served as electrochemical sensing platforms and carrier of signal materials to amplify reaction signal. In addition, HRP-Ab<sub>2</sub>-SiO<sub>2</sub> NSs bioconjugate catalyzed the reduction of H<sub>2</sub>O<sub>2</sub> in the presence of thionine, further amplifying the reaction signal. The research results showed that the immunosensor exhibited high sensitivity and provided a promising potential in clinical applications.

#### ACKNOWLEDGMENTS

The authors acknowledged financial support from Anhui Provincial Natural Science Foundation (1908085MH272), The Research Fund for University Natural Science Research Project of Anhui Province (KJ2021A0842), National Natural Foundation of China (21645006), The Young Research Fund of Wannan Medical College (WK201917) and Health Commission Science Research Project of Anhui Province (AHWJ2021b035).

## References

1. C. Dejous and U. M. Krishnan, *Biosens. Bioelectron.*, 173(2021)112790.
2. C. Ibaú, M. K. Md-Arshad and S. C. B. Gopinath, *Biosens. Bioelectron.*, 98(2017)267.
3. A. Shamsazar, A. Asadi, D. Seifzadeh and M. Mahdavi, *Sens. Actuat. B: Chem.*, 346 (2021) 130459.
4. Y. B. Wang, M. Y. Wang, H. P. Yu, G. Wang, P. X. Ma, S. Pang, Y. M. Jiao and A. H. Liu, *Sens. Actuat. B: Chem.*, 367(2022) 132009.
5. D. C. Pérez-Ibave, C. H. Burciaga-Flores and M. N. Elizondo-Riojas, *Cancer. Epidemiol.*, 54(2018) 48.
6. V. P. Hendrik, M. J. Roobol, C. R. Chapple, J. W. F. Catto, J. N'Dow, J. Sønksen, A. Stenzl and M. Wirth, *Eur. Urol.*, 9477(2021)1.
7. Y. C. Chen, M. J. Ruan, B. Y. Zhou, X. G. Hu, H. Wang, H. Liu, J. Liu and G. Song, *Clin. Genitourin. Canc.*, 19(2021)288.
8. F. Martínez-Rojas, E. Castañeda and F. Armijo, *J. Electroanal. Chem.*, 880 (2021) 114877.
9. H. Ehzari, M. Amiri and M. Safari, *Talanta*, 210 (2020) 120641.
10. C. Özyurt, İ. Uludağ, B. İnce and M. K. Sezgintürk, *J. Pharmaceut. Biomed.*, 209(2022)114535.
11. Y. L. Sun, P. Gao, R. Han, C. N. Luo and Q. Wei, *Sens. Actuat. B: Chem.*, 333(2021) 129543.
12. J. H. He, Y. Y. Cheng, Q. Q. Zhang, H. Liu and C. Z. Huang, *Talanta*, 219 (2020)121276.
13. X. L. Wang, X. Y. He, Z. H. He, L. W. Hou, C. Ge, L. Wang, S. B. Li and Y. Xu, *Biosens. Bioelectron.*, 204(2022)114057.
14. X. Q. Li, F. H. Ma, M. H. Yang and J. L. Zhang, *Mater. Today. Adv.*, 14(2022)100219.
15. F. Farshchi and M. Hasanzadeh, *Biomed. Pharmacother.*, 132(2020)110878.
16. M. Barani, F. Sabir, A. Rahdar, R. Arshad and G. Z. Kyzas, *Nanomaterials*, 10(2020)1696.
17. M. Azharuddin, G. H. Zhu, D. Das, E. Ozgur, L. Uzun, A. P. F. Turner and H. K. Patra, *Chem. Commun.*, 55(2019)6964.
18. P. M. Martins, A. C. Lima, S. Ribeiro, S. Lanceros-Mendez and P. Martins, *ACS. Appl. Bio. Mater.*, 4(2021)5839.
19. Y. Chen, W. R. Chu, W. Liu, X. Y. Guo, Y. Jin and B. X. Li, *Microchim Acta.*, 185 (2018)187.
20. F. Ma, C. C. Li and C. Y. Zhang, *J. Mater. Chem.*, 6(2018)6173.
21. L. H. Li, D. X. Feng, J. Q. Zhao, Z. L. Guo and Y. Z. Zhang, *RSC. Adv.*, 5(2015)105992.
22. D. P. Tang, Y. L. Cui and G. N. Chen, *Analyst*, 138(2013)981.
23. X. H. Lin, A. O. Beringhs and X. L. Lu, *AAPS. J.*, 43(2021)1550.
24. A. A. Nayl, A. I. Abd-Elhamid, A. A. Alyc and S. Bräsede, *RSC. Adv.*, 22(2022),13706.
25. J. N. Fan, Y. Q. Cheng and M. T. Sun, *Chem. Rec.*, 20(2020)1474.
26. N. Díez, M. Sevilla and A. B. Fuerte, *Mater. Today. Nano.*, 16(2021)100147.
27. D. X. Feng, L. H. Li, X. Fang, X. W. Han and Y. Z. Zhang, *Electrochimica Acta.*, 127 (2014) 334.
28. J. Huang, H. Wang, D. P. Li, W. Q. Zhao, L. Y. Ding and Y. Han, *Mater. Sci. Eng.*, 31(2011)1374.
29. Y. Vida, M. I. Montanez, D. Collado, F. Najera, A. Ariza, M. Blanca, M. J. Torres, C. Mayorga and E. Perez-Inestrosa, *J. Mater. Chem.*, 1(2013)3044.
30. L. H. Li, D. X. Feng and Y. Z. Zhang, *Anal. Biochem.*, 505 (2016) 59.
31. M. Li, F. Cheng, C. Y. Xue, H. Q. Wang, C. Chen, Q. Q. Du, D. Ge and B. B. Sun, *Langmuir*, 35(2019)4688.
32. L. H. Li, Y. Wei, S. P. Zhang, X. S. Chen, T. L. Shao and D. X. Feng, *Electroanal. Chem.*, 880(2021)114882.
33. R. Wang, W. D. Liu, A. J. Wang, Y. D. Xue, L. Wu and J. J. Feng, *Biosens. Bioelectron.*, 99 (2018) 458.
34. L. Talamini, N. Zanato, E. Zapp, D. Brondani, E. Westphal, H. Gallardo and I. C. Vieira, *Electroanal*, 30(2018)353.

35. L. Yu, Z. Fan, W. X. Li, S. Q. Li, P. T. Wang and H. Q. Wang, *Int. J. Electrochem. Sci.*, 12 (2017) 8188.
36. L. Suresh, P. K. Brahman, K. R. Reddy and J. S. Bondili, *Enzyme. Microb. Tech.*, 112(2018) 43.
37. M. Ghanavati, F. Tadayon and H. Bagheri, *Microchem. J.*, 159(2020)105301.
38. M. Sajadpour, S. Abbasian, H. Siampour, H. Bagheri and A. Moshaii, *J. Solid. State. Electrochem.*, 26 (2022)149.
39. K. Zhang, Z. W. Cao, S. Z. Wang, J. X. Chen, Y. Wei and D. X. Feng, *Int. J. Electrochem. Sci.*, 15 (2020) 2604.

© 2022 The Authors. Published by ESG ([www.electrochemsci.org](http://www.electrochemsci.org)). This article is an open access article distributed under the terms and conditions of the Creative Commons Attribution license (<http://creativecommons.org/licenses/by/4.0/>).